Preparative and Electrochemical Investigations on the Electron Sponge Behavior of Cobalt Telluride Clusters: CO Substitution in $[Co_{11}Te_7(CO)_{10}]^{n-}$ Ions ($n = 1, 2$) by PMe_2Ph and Crystal Structure of $[Co_{11}Te_7(CO)_5(PMe_2Ph)_5]$

Henri Brunner,[a] Hélène Cattey,[b] Walter Meier,[a] Yves Mugnier,[b] A. Claudia Stückl,[c] Joachim Wachter,*[a] Robert Wanninger,[a] and Manfred Zabel[a]

Abstract: The reaction of the cluster salts $[Cp^*_2Nb(CO)_2]_n[Co_{11}Te_7(CO)_{10}]$ ($Cp^* = C_5Me_5$; $n = 1$, 2) with excess PMe_2Ph gave the neutral, dark brown clusters $[Co_{11}Te_7(CO)_6(PMe_2Ph)_4]$ (**5**) and $[Co_{11}Te_7(CO)_5(PMe_2Ph)_5]$ (**6**) with 147 metal valence electrons. The new compounds were characterized by IR spectroscopy, elemental analyses, and mass spectrometry. The molecular structure of **6** was determined by X-ray crystallography. Like its precursor anion, it consists of a pentagonal-prismatic $[Co_{11}Te_7]$ core, but with a ligand sphere composed of five CO and five PMe_2Ph ligands. Detailed electrochemical studies of both reactions reveal that a stepwise substitution of CO ligands in the initial cluster anions takes place leading to intermediate $[Co_{11}Te_7(CO)_{10-m}(PMe_2Ph)_m]^{n-}$ ions ($m = 1-5$; $n = 1$, 2). Each of these intermediates is distinguished by at least one oxidation and two reduction waves, giving rise to a total of 21 redox couples and 27 electroactive species. The electron sponge character of the new compounds is particularly pronounced in **5**, which exhibits charges n between $+1$ and -4 corresponding to metal valence electron counts of between 146 and 151.

Keywords: carbonyl ligands · cluster compounds · cobalt · electrochemistry · tellurium

Introduction

Recent developments in the coordination chemistry of tellurium-derived ligands[1] focus on their ability for cluster aggregation.[2] In this context transition-metal telluride clusters are important links between molecular and solid-state compounds.[3] Comparatively little effort has been made to investigate the reactivity of metal-rich telluride clusters bearing additional ligands such as CO groups. Little is known about the redox chemistry of such metal carbonyl telluride clusters.[4] In these compounds a polymetallic core is held together by comparatively few telluride ligands, thus one may expect electron-sink features similar to those in homoleptic metal carbonyl clusters.[5]

The cluster anions $[Co_{11}Te_7(CO)_{10}]^{n-}$ ($n = 1$: $[\mathbf{1}]^-$; $n = 2$: $[\mathbf{1}]^{2-}$) are metal telluride clusters with considerable metallic interactions within the cluster core.[6] They are part of the saltlike compounds $[Cp^*_2Nb(CO)_2]_n[Co_{11}Te_7(CO)_{10}]$ ($Cp^* = C_5Me_5$; $n = 1$, 2), which form in the reaction of $[Cp^*_2Nb(Te_2H)]$ with $[Co_2(CO)_8]$.[6] Their structures are characterized by a body-centered pentagonal-prismatic Co_{11} skeleton (Figure 1);[6, 7] the seven faces of the prism are

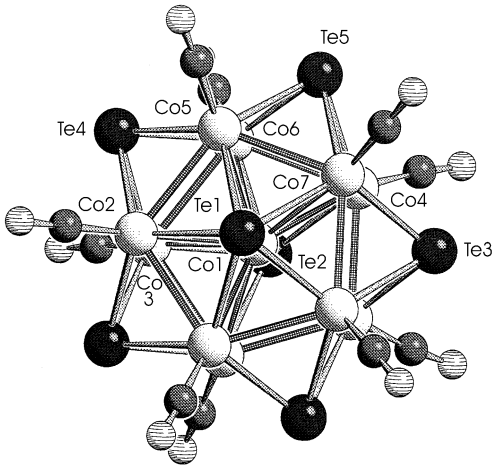

Figure 1. Structure of $[Co_{11}Te_7(CO)_{10}]^-$ ($[\mathbf{1}]^-$) (view down the C_5 axis).[6]

[a] Dr. J. Wachter, Prof. Dr. H. Brunner, W. Meier, Dr. R. Wanninger, Dr. M. Zabel
Institut für Anorganische Chemie der Universität Regensburg
93040 Regensburg (Germany)
Fax: (+49) 941-943-4439
E-mail: Joachim.Wachter@chemie.uni-regensburg.de

[b] Dr. H. Cattey, Prof. Y. Mugnier
Laboratoire de Synthèse et d'Electrosynthèse
Organométalliques (UMR 5682)
Université de Bourgogne
21100 Dijon (France)

[c] Dr. A. C. Stückl
Institut für Anorganische Chemie
Georg-August-Universität Göttingen
37077 Göttingen (Germany)

DOI: 10.1002/chem.200304841

bridged by five μ_4- and two μ_5-Te ligands, respectively. Both cluster anions are in a redox relationship to each other and two further derivatives with $n=0$ (**1**) and $n=3$ ($[\mathbf{1}]^{3-}$) have been established by electrochemical methods and density functional theory (DFT) studies.[6] Herein we report on the consecutive substitution of up to five CO groups by PMe_2Ph in the cluster skeleton. Electrochemical studies reveal a series of potential intermediates and electron transfer processes.

Results

Syntheses, properties and structural characterization: The reaction of $[Cp^*_2Nb(CO)_2][Co_{11}Te_7(CO)_{10}]$ with an excess of PMe_2Ph in CH_2Cl_2 or THF at room temperature gave, after chromatography on silica gel, the neutral, dark brown compound $[Co_{11}Te_7(CO)_6(PMe_2Ph)_4]$ (**5**) in good yield [Eq. (1)]. Starting from $[Cp^*_2Nb(CO)_2]_2[Co_{11}Te_7(CO)_{10}]$, compound **5** was obtained along with another dark brown cluster, which, which was isolated by fractional crystallization and analyzed as $[Co_{11}Te_7(CO)_5(PMe_2Ph)_5]$ (**6**) [Eq. (1)].

$$\left.\begin{array}{l}[Cp^*_2Nb(CO)_2][Co_{11}Te_7(CO)_{10}]\\ [Cp^*_2Nb(CO)_2]_2[Co_{11}Te_7(CO)_{10}]\end{array}\right\} \xrightarrow[-\,CO]{L = PMe_2Ph} \begin{array}{l}[Co_{11}Te_7(CO)_6L_4]\ \mathbf{5}\\ +\\ [Co_{11}Te_7(CO)_5L_5] + \ldots\ \mathbf{6}\end{array} \qquad (1)$$

Electrochemical investigations on the system $[Cp^*_2Nb(CO)_2][Co_{11}Te_7(CO)_{10}]/PMe_2Ph$ (see below) have shown that potential intermediates may be derived by a consecutive substitution of CO ligands by PMe_2Ph ligands in the anionic cluster skeleton [Eq. (2)]. Unfortunately, it has been impossible to separate and crystallize the corresponding salts. Instead, chromatography of the resulting mixtures allowed the isolation of neutral compounds relatively rich in phosphane ligands. Attempts to control the formation of intermediate clusters such as $[Co_{11}Te_7(CO)_9(PMe_2Ph)]$ (**2**) and $[Co_{11}Te_7(CO)_8(PMe_2Ph)_2]$ (**3**) by employing the corresponding stoichiometric amounts of PMe_2Ph failed. Accidentally, it was possible in one case to isolate $[Co_{11}Te_7(CO)_7(PMe_2Ph)_3]$ (**4**), which was identified by its mass spectrum and then subjected to electrochemical investigations (see below).

$$\begin{array}{l}[Co_{11}Te_7(CO)_{10}]^- \xrightarrow[-\,CO]{L} [Co_{11}Te_7(CO)_9L]^- \xrightarrow[-\,CO]{L} [Co_{11}Te_7(CO)_8L_2]^- \xrightarrow[-\,CO]{L}\\ \quad\mathbf{[1]^-}\qquad\qquad\quad\mathbf{[2]^-}\qquad\qquad\quad\mathbf{[3]^-}\\ \qquad\qquad [Co_{11}Te_7(CO)_7L_3]^- \xrightarrow[-\,CO]{L} [Co_{11}Te_7(CO)_6L_4]^-\\ L = PMe_2Ph\qquad\qquad\quad\mathbf{[4]^-}\qquad\qquad\quad\mathbf{[5]^-}\end{array} \qquad (2)$$

Compounds **5** and **6** are soluble in toluene, dichloromethane, and acetone and give correct elemental analyses. The field desorption mass spectra of **5** and **6** exhibit the parent ions. This is consistent with the substitution of four and five CO groups, respectively, by PMe_2Ph. This behavior is in striking contrast to that of the parent cluster anions, which do not exhibit any mass spectra at all. The observed and simulated isotope patterns for the parent ion of $[Co_{11}Te_7(CO)_6(PMe_2Ph)_4]$ (**5**) are shown in Figure 2.

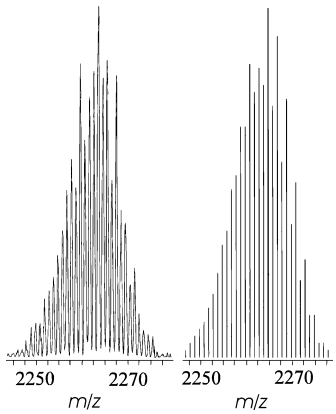

Figure 2. Molecular peak in the FD mass spectrum of **5** (left) and simulated spectrum (right).

The IR spectrum of **5** exhibits one strong and relatively broad absorption between 1942 and 1930 cm^{-1}, whereas two absorptions at 1909 and 1931 cm^{-1} are observed for **6**. These bands are typical of terminal CO ligands, which are distributed over the pentagonal-prismatic $Co_{11}Te_7$ core of the respective compounds. Compared to the parent cluster anions $[Co_{11}Te_7(CO)_{10}]^{n-}$ ($n=1$, 2) they are slightly shifted towards lower wavenumbers indicating an increase of electron density in the cluster core by the incoming substituents. Each compound also contains absorptions typical of the phosphine ligands, whereas the weak but characteristic CH absorptions of the $[Cp^*_2Nb(CO)_2]^+$ ions have disappeared.

Although recrystallization of **5** from different solvents gave dark brown prisms of well-defined shape they did not diffract X-ray radiation at all. For compound **6**, however, flat prisms were obtained which were suitable for an X-ray structure analysis. Although the structure solution was handicapped by intergrowth problems leading to relatively high R_{int} values, the result is reliable as far as the heavy-atom skeleton is concerned. The structure makes also sense if it is compared with the structure of the precursor anion $[Co_{11}Te_7(CO)_{10}]^-$ (Figure 1).

The molecular structure of **6** contains a pentagonal prism of ten cobalt atoms, and a further Co atom resides in the center of this prism (Figure 3 and Figure 4). While the five square faces are capped by μ_4-Te ligands, both pentagonal faces are capped by μ_5-Te ligands. The Co_{10} prism bears five CO and

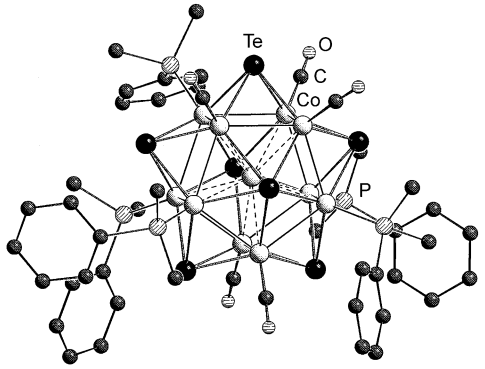

Figure 3. Molecular structure of **6** (top view).

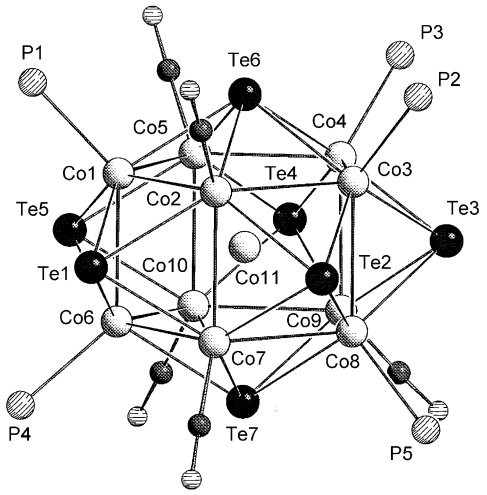

Figure 4. $Co_{11}Te_7(CO)_5P_5$ core of **6** in side view with labeling scheme.

five PMe_2Ph ligands. The phosphane ligands "P1" and "P4" as well as "P2" and "P5" are found in an eclipsed conformation with respect to the five-membered Co faces. The existence of further positional isomers may be possible, but this cannot be verified by NMR spectroscopy because of the paramagnetic nature of the compound.

The bond parameters of the four structural units [μ_5-Te–Co, μ_4-Te–Co, Co–Co, Co–Co11] are comparable to those in the parent cluster ion $[\mathbf{1}]^-$ (Table 1). All Co–Te and Co–Co bond lengths are approximately of equal order so that nearly perfectly edge-sharing octahedra are arranged around the central Te6-Co11-Te7 axis. This means that the loss of fivefold symmetry during the reaction and the replacement of five π-acceptor CO ligands by phosphane donors does not affect the cluster geometry in a significant manner. A comparison of the bond parameters of **6** with those of $[Co_{11}Te_7(CO)_{10}]^-$[6] and $[Co_{11}Te_7(CO)_{10}]^{2-}$[7] shows that deviations are at the limit of accuracy of the crystal structure determinations (Table 2). This may indicate that oxidation of the cluster core may be sufficiently compensated by delocalization of the skeletal electrons and by an increase of electron density from the new σ-donor ligands.

Table 2. Comparison of important distances [Å] of $[\mathbf{1}]^-$,[6] $[\mathbf{1}]^{2-}$,[7] and **6**.

	6	$[\mathbf{1}]^-$	$[\mathbf{1}]^{2-}$
μ_4-Te–Co	2.499(2) – 2.545(2)	2.498(3) – 2.523(3)	2.510(2)[b]
μ_5-Te–Co	2.550(2) – 2.599(2)	2.552(3) – 2.581(3)	2.569(2)[b]
Te–Co_{bc}[a]	2.646(2), 2.673(2)	2.631(3), 2.649(3)	2.642(2), 2.647(2)
Co–Co	2.546(2) – 2.655(2)	2.522(4) – 2.612(4)	2.602(4)[b]
Co–Co_{bc}[a]	2.532(2) – 2.583(2)	2.544(4) – 2.572(3)	2.558(3)[b]
Co–C[b]	1.75(1)	1.75(2)	1.76(1)

[a] Body-centered Co. [b] Average values.

The metal valence electron (MVE) count for **6** is 147 MVE, whereas the cluster cores of the $[\mathbf{1}]^{n-}$ ions either contain 149 ($n=2$) or 148 MVE ($n=1$). The relative stability of these anions has been calculated by density functional theory (DFT) methods.[6] Thus, from bonding energy calculations they are by about 2 kcal mol^{-1} more stable than the unsubstituted 147 MVE species $[Co_{11}Te_7(CO)_{10}]^0$ (**1**). First hints for the possible existence of **1** have been obtained by electrochemical oxidation of $[\mathbf{1}]^-$.[6] From the actual results one may conclude that PMe_2Ph is able to stabilize neutral clusters of the type $[Co_{11}Te_7(CO)_{10-m}(PMe_2Ph)_m]$ ($m=4$, 5) by CO substitution and electron transfer.

Preliminary results obtained with L = PMe_3, $P(OMe)_3$, and PPh_3 show that this reaction type may be extended to the formation of other $[Co_{11}Te_7(CO)_6L_4]$ clusters.[8] However, detailed investigations, particularly concerning electrochemical behavior of these products, are still in progress.

Electrochemical investigations: To understand both the successive substitution of CO by PMe_2Ph and the participating electron transfer reactions, electrochemical investigations were carried out. The reactions of $[Cp_2^*Nb(CO)_2]_n[Co_{11}Te_7(CO)_{10}]$ ($n=1$, 2) with PMe_2Ph were studied in different stoichiometries. In agreement with our previous work the rotating disk electrode (RDE) voltammogram of $[Cp_2^*Nb(CO)_2][Co_{11}Te_7(CO)_{10}]$ exhibits one oxidation wave E_1' and four reduction waves A_1, B_1, C_1, and D_1.[6] In this study only the reduction waves A_1 and B_1 are considered (Figure 5), for C_1 and D_1, which

Table 1. Selected bond lengths [Å] and angles [°] for $[Co_{11}Te_7(CO)_5(PMe_2Ph)_5]$ (**6**).

P1–Co1	2.1770(19)	P2–Co3	2.215(2)	P3–Co4	2.206(3)
P4–Co6	2.180(2)	P5–Co8	2.182(2)	Co1–Te1	2.5297(11)
Co1–Te5	2.5137(9)	Co1–Te6	2.5580(11)	Co1–Co2	2.5769(12)
Co1–Co5	2.5769(13)	Co1–Co6	2.5676(14)	Co1–Co11	2.5432(12)
Co2–Te1	2.5062(11)	Co2–Te2	2.5232(10)	Co2–Co3	2.5531(13)
Co2–Co11	2.5673(12)	Co2–Te6	2.5751(12)	Co2–Co7	2.6159(14)
Co3–Te3	2.5121(10)	Co3–Te2	2.5156(12)	Co3–Te6	2.5812(10)
Co3–Co11	2.5831(12)	Co3–Co8	2.6084(14)	Co3–Co4	2.6402(13)
Co4–Te3	2.5138(10)	Co4–Te4	2.5223(10)	Co4–Co11	2.5576(15)
Co4–Te6	2.5592(10)	Co4–Co5	2.5847(13)	Co4–Co9	2.6547(15)
Co5–Te4	2.5143(10)	Co5–Te5	2.5190(12)	Co5–Co11	2.5609(13)
Co5–Te6	2.5868(10)	Co5–Co10	2.6447(14)	Co6–Te5	2.5069(10)
Co6–Te1	2.5075(9)	Co6–Co11	2.5387(14)	Co6–Co10	2.5517(13)
Co6–Co7	2.5615(12)	Co6–Te7	2.5934(9)	Co7–Te2	2.5021(10)
Co7–Te1	2.5119(9)	Co7–Te7	2.5496(9)	Co7–Co11	2.5658(14)
Co7–Co8	2.5741(13)	Co8–Te2	2.5002(10)	Co8–Co11	2.5315(12)
Co8–Te3	2.5354(12)	Co8–Co9	2.5462(13)	Co8–Te7	2.5798(10)
Co9–Te4	2.4989(11)	Co9–Te3	2.5453(11)	Co9–Co11	2.5472(12)
Co9–Te7	2.5992(12)	Co9–Co10	2.6122(13)	Co10–Te4	2.5086(12)
Co10–Te5	2.5330(10)	Co10–Co11	2.5425(12)	Co10–Te7	2.5688(11)
Co11–Te6	2.6458(11)	Co11–Te7	2.6729(11)	Co–C_{mean}	1.75(1)
P1-Co1-Te1	102.16(7)	Te1-Co1-Te5	109.78(4)	P1-Co1-Co11	164.00(8)
Te1-Co1-Co11	87.75(4)	Te1-Co1-Te6	118.97(3)	P1-Co1-Co6	136.39(8)
Te6-Co1-Co6	122.05(4)	P1-Co1-Co2	114.33(6)	Te1-Co1-Co5	144.86(4)
Te1-Co1-Co2	58.78(3)	Co2-Co1-Co5	108.98(4)		

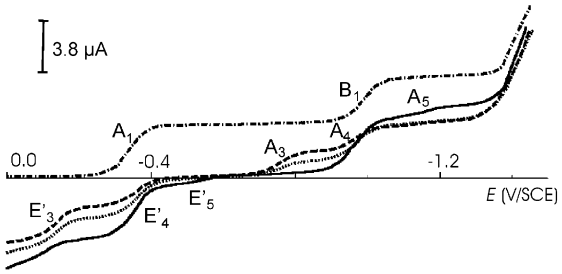

Figure 5. Part of the RDE voltammogram of $[Cp^*_2Nb(CO)_2][Co_{11}Te_7(CO)_{10}]$ on a carbon electrode in THF (0.2 M NBu_4PF_6): initial (•–•–); after adding 7 equivalents of PMe_2Ph (– – –), 14 equivalents of PMe_2Ph (••••) and after 2 h (——).

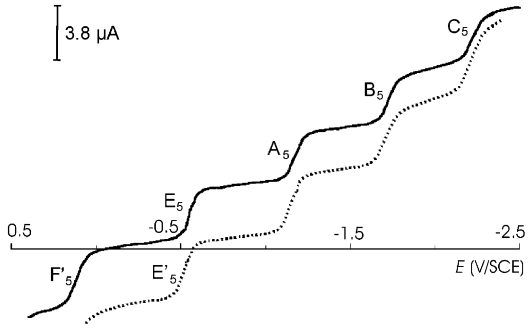

Figure 6. RDE voltammogram of **5** on carbon electrode in THF (0.2 M NBu_4PF_6): initial (——) and after electrolysis at -0.7 V (••••).

are not shown, correspond to the reduction of the cation $[Cp^*_2Nb(CO)_2]^+$.

After the addition of seven equivalents of PMe_2Ph to the solution of $[Cp^*_2Nb(CO)_2][Co_{11}Te_7(CO)_{10}]$ in THF, which contains $[\mathbf{1}]^-$ as the electrochemically relevant species, an immediate evolution is observed (Figure 5). Reduction waves A_1 and B_1 disappear to the profit of new oxidation waves E'_4 ($E_{1/2} = -0.36$ V) and E'_3 ($E_{1/2} = -0.12$ V) and new reduction waves A_3 ($E_{1/2} = -0.76$ V) and A_4 ($E_{1/2} = -0.98$ V). The heights of E'_3 and A_3 as well as of E'_4 and A_4 are equal. After addition of a large excess of PMe_2Ph (14 equiv), the heights of waves E'_3 and A_3 decrease, whereas waves E'_4 and A_4 increase. After two hours, two additional weak waves E'_5 (oxidation) and A_5 (reduction) appear. The potential difference between waves A_1 and A_3 ($\Delta = 0.44$ V) is about twice as high as the difference between A_3 and A_4 ($\Delta = 0.22$ V) and between A_4 and A_5 ($\Delta = 0.18$ V).

These results are tentatively interpreted in terms of a stepwise CO substitution in initial $[\mathbf{1}]^-$ by PMe_2Ph. Thus, in a first step the monosubstituted anion $[Co_{11}Te_7(CO)_9(PMe_2Ph)]^-$ ($[\mathbf{2}]^-$) may form in a fast reaction. Under the given reaction conditions (excess phosphane) this species may be converted rapidly into disubstituted $[Co_{11}Te_7(CO)_8(PMe_2Ph)_2]^-$ ($[\mathbf{3}]^-$), which is characterized by the waves E'_3 and A_3. The new couples A_4/E'_4 and A_5/E'_5, which may be assigned to the tri- and tetrasubstituted derivatives $[Co_{11}Te_7(CO)_7(PMe_2Ph)_3]^-$ ($[\mathbf{4}]^-$)[9] and $[Co_{11}Te_7(CO)_6(PMe_2Ph)_4]^-$ ($[\mathbf{5}]^-$), respectively, appear after 2 h [Eq. (2)].

From Figure 5 one may also conclude that the substitution of one CO group by PMe_2Ph renders the substitution products more difficult to be reduced (and consequently more easily oxidizable). On the other hand, an excess of PMe_2Ph provoques slow formation of the waves A_5 and E'_5, which may be assigned to the tetrasubstituted $[\mathbf{5}]^-$ (see below). Whereas waves A_5 and E'_5 are only of low intensity after 2 h, a continuous decrease of waves A_4 and E'_4 in favor of A_5 and E'_5 has been observed after 17 h. Additionally, a new couple A_6/E'_6, characteristic of pentasubstituted $[\mathbf{6}]^-$, appears at $E_{1/2} = -0.74$ and -1.36 V.

Our hypotheses have been verified by the electrochemical study of chemically prepared **5** [Eq. (1)]. Its voltammogram (Figure 6) shows one oxidation wave at F'_5 ($E_{1/2} = 0.10$ V) and four reduction waves E_5, A_5, B_5, and C_5 at $E_{1/2} = -0.54$, -1.16, -1.71, and -2.05 V, respectively. The heights of all these waves are nearly equal, and each corresponds to a one-electron transfer. By cyclic voltammetry, five reversible systems were obtained. Half-wave potentials were found to increase independently of scan rate and peak current and linearly with $\nu^{1/2}$. For each reduction step, the potential gap between the anodic and cathodic peaks is close to 50 mV at scan rates up to 0.2 V s^{-1}. The values are in agreement with the theoretical values for diffusion-controlled one-electron transfer and this was verified by controlled potential electrolysis at -0.7 V (E_5 plateau), which gave 1.0 ± 0.1 electrons for the reduction step. The resulting cluster anion $[\mathbf{5}]^-$, which is obtained quantitatively, is characterized by the oxidation wave E'_5 and three reduction waves A_5, B_5, and C_5 (Figure 6). These systems are reversible. Of particular interest is the wave C_5/C'_5 ($E_{1/2} = -2.05$ V), which may indicate the possible existence of the highly charged anion $[\mathbf{5}]^{4-}$.

A crystalline sample of $[Co_{11}Te_7(CO)_5(PMe_2Ph)_5]$ (**6**) was also subjected to electrochemical studies. One oxidation wave F'_6 and three reduction waves E_6, A_6, B_6 have been obtained by RDE (Figure 7a). The heights of all these waves are nearly

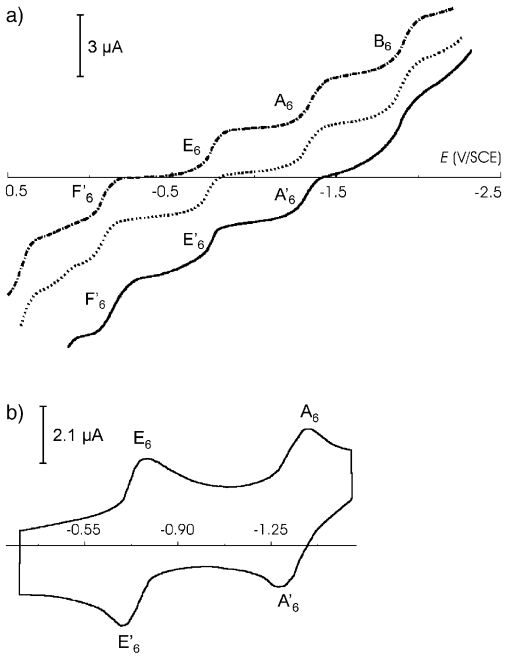

Figure 7. a) RDE voltammogram of **6** on a carbon electrode in THF (0.2 M NBu_4PF_6): initial (•–•–); after electrolysis at -1 V (••••); after a new electrolysis at -1.5 V (——). b) Cyclic voltammogram of **6** (THF/0.2 M NBu_4PF_6; scan rate 0.1 V s^{-1}).

equal and each correspond to a one-electron transfer. By cyclic voltammetry, three reversible systems F'_6/F_6, E_6/E'_6 and A_6/A'_6 were observed. These systems exhibit the usual characteristics of one-electron transfer steps as described above. Figure 7b shows the cyclovoltammograms of the systems E_6/E'_6 and A_6/A'_6. The reversibility of the systems E_6/E'_6 and A_6/A'_6 was also verified by controlled potential electrolysis. After reduction at -1 V (E_6 plateau), one electron is consumed ($n_{exp} = 0.84\ e^-$), giving rise to the formation of the anionic cluster $[\mathbf{6}]^-$. The resulting RDE voltammogram exhibits two oxidation waves F'_6 and E'_6 and two reduction waves A_6 and B_6. By electrolysis at -1.5 V (A_6 plateau) and consumption of one further electron ($n_{exp} = 1.1\ e^-$) $[\mathbf{6}]^{2-}$ may have been formed, which shows the oxidation waves A'_6, E'_6, F'_6 and the reduction wave B_6 (Figure 7a). In contrast, the system B_6/B'_6 shows partial irreversibility, due to apparent instability of the electrogenerated species $[\mathbf{6}]^{3-}$.

It has already been demonstrated in Figure 5 that the system $[\mathbf{1}]^-/PMe_2Ph$ shows a continuous evolution towards higher substituted clusters. This fact makes it very difficult to isolate the pure mono- or disubstituted clusters on the preparative scale even if a 1:1 stoichiometry is employed. Instead, the formation of a mixture was observed consisting of mono-, di-, and trisubstituted clusters along with unreacted starting material.

To get information on the influence of the charge of the initial cluster anion on the reaction rates the system $[Cp^*_2Nb(CO)_2]_2[Co_{11}Te_7(CO)_{10}]/PMe_2Ph$ was electrochemically studied. The RDE voltammogramm of the part corresponding to $[\mathbf{1}]^{2-}$ reveals two oxidation waves E'_1 (not considered here) and A'_1 and one reduction wave B_1 at $E_{1/2} = -1.04$ V (Figure 8).[6] Addition of dimethylphenylphosphane to the solution results in a slow diminution of the two

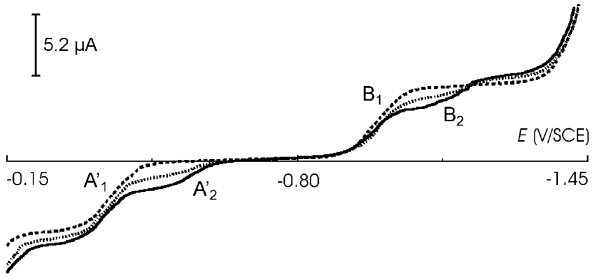

Figure 8. Part of the RDE voltammogram of $[Cp^*_2Nb(CO)_2]_2[Co_{11}Te_7(CO)_{10}]$ on a carbon electrode in THF (0.2 M NBu_4PF_6): initial (– – –); after adding 14 equivalents of PMe_2Ph (••••) and after 2 h (——).

waves A'_1 and B_1. In contrast to the system $[\mathbf{1}]^-/PMe_2Ph$ (Figure 5), the two waves A'_2 and B_2 are observed after 2 h. These waves with $E_{1/2} = -0.53$ V (A'_2) and -1.16 V (B_2) may be typical of a slow monosubstitution of $[Co_{11}Te_7(CO)_{10}]^{2-}$ and the subsequent redox processes of the resulting $[Co_{11}Te_7(CO)_9(PMe_2Ph)]^{2-}$ ($[\mathbf{2}]^{2-}$).

Finally, the overall reactivity of the investigated system may be summarized in Scheme 1, in which 21 redox couples and 27 electroactive species are specified. The electron transfer reactions are written horizontally and the substitution reactions (CO by PMe_2Ph) vertically. The potential difference between E_p/E'_p and A_p/A'_p systems ($p = 1-6$) is equal to about 0.6 V, and the difference between A_p/A'_p and B_p/B'_p systems ($p = 1-6$) is equal to 0.7 V. This reflects the fact that all the clusters have rather similar redox properties. The CO substitution by a PMe_2Ph group, which is a better σ donor ligand than CO, renders reduction more difficult and oxidation easier. Additionally, each CO substitution step causes a shift of about 200 mV towards negative potential.

Discussion

This study focuses on the substitution of CO ligands from a cobalt telluride framework of the rare pentagonal-prismatic structure type. The cluster salts $[Cp^*_2Nb(CO)_2]_n[Co_{11}Te_7(CO)_{10}]$ ($n = 1$, 2) form with PMe_2Ph neutral clusters of composition $[Co_{11}Te_7(CO)_{10-m}(PMe_2Ph)_m]$ ($m = 4$, 5), regardless of the charge of the initial cluster anions. The substitution reaction is accompanied by an oxidation of the cluster core, for example from 149 metal valence electrons (MVE) in $[Co_{11}Te_7(CO)_{10}]^{2-}$ to 147 MVE in **5**. The substitution of CO ligands in the negatively charged cluster core is somewhat unexpected if one considers that in the $[Cp^*_2Nb(CO)_2]^+$ ion the substitution of at least one CO group should be facilitated by the positive charge at the metal center. However, there is still no proof for a substitution of a CO ligand in this cation and its fate is unknown. In a control experiment we have shown that $[Cp^*_2Nb(CO)_2][Co(CO)_4]$,[6] dissolved in CH_2Cl_2, does not react with PMe_2Ph under analogous conditions.

Electrochemical studies of the reaction reveal that the substitution of CO groups is a stepwise process, in which differently substituted cluster anions $[Co_{11}Te_7(CO)_{10-m}(PMe_2Ph)_m]^{n-}$ ($m = 1-5$, $n = 1$, 2) are formed as intermediate products. Each of these intermediates exhibits at least three electron transfer processes, leading to a total of 21 redox couples with 27 electroactive species. A further characteristic within the substitution row from low to high m is a systematic shift of the respective potentials towards more negative values by the incoming PMe_2Ph ligand.

In DFT calculations on $[\mathbf{1}]^{n-}$ ($n = 1$, 2) it has been argued that the interactions between the Co atoms are close to metallic.[6] The redox behavior of the unsubstituted cluster anions may also be influenced by this *quasi-metallic* behavior of the cluster entity with respect to the electron distribution. Among other reasons, in the new compounds the increasing number of phosphane ligands with σ-donor capacities provokes an increase of electron density in the cluster core. Additionally, the stabilization of the Co_{11} cage orbitals is due to the significant loss in symmetry by substitution: the idealized neutral model cluster $[Co_{11}Te_7(CO)_9(PH_3)]$ is of C_s symmetry compared to D_{5h} in the unsubstituted case. Preliminary calculations show that even though this symmetry reduction is not reflected by the Co and Te positions of the X-ray diffraction study of **6**, a very different picture of the node planes is found by an analysis of the MO coefficients. As far as the highest occupied molecular orbital (HOMO) is concerned, a relatively strong orbital mixing was obtained for this singly occupied MO. The contribution of the d states of

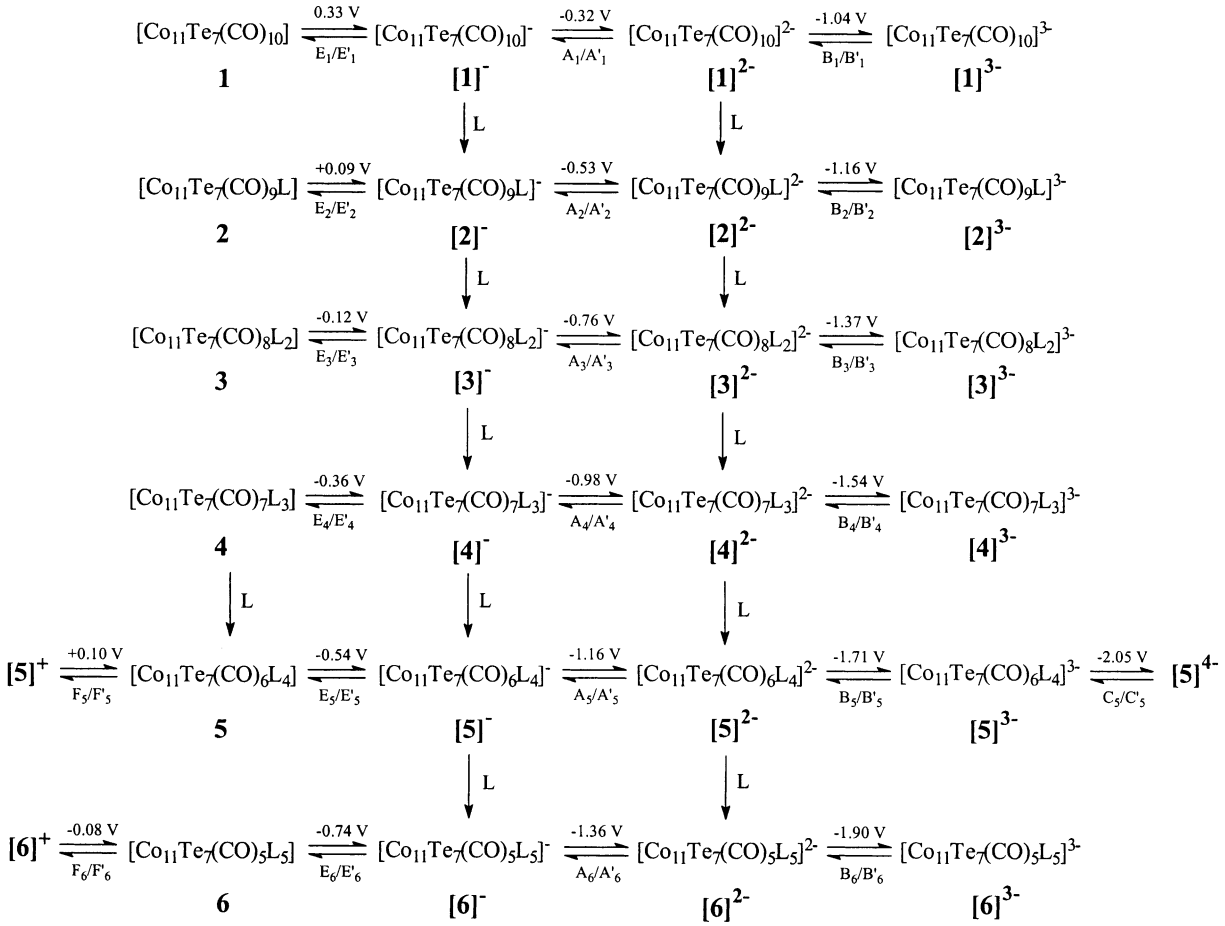

Scheme 1. Global presentation of the reaction of $[Cp^*_2Nb(CO)_2][Co_{11}Te_7(CO)_{10}]$ with L = PMe_2Ph: Verified redox couples (horizontal) and CO substitution steps (vertical).

the ten cluster cage Co atoms to the HOMO is significantly increased, and the body-centered Co mainly participates by a distorted $d_{x^2-y^2}$ orbital. The characteristics of the LUMO resemble those of the LUMO of $[\mathbf{1}]^-$. These properties may even be more pronounced in the case of larger degrees of substitution, for example the electron sponge behavior of the highly substituted cluster **5**. Thus, the distinct charges of the $Co_{11}Te_7$ cluster core of **5** range between $n=+1$ and $n=-4$, corresponding to numbers of MVEs of between 146 in $[\mathbf{5}]^+$ and 151 in $[\mathbf{5}]^{4-}$.

Whereas the electrochemical pathways seem to be clear, the bulk synthesis of the neutral clusters **5** and **6** raises the question of the origin of the final oxidizing step. Each replacement of a CO ligand by PMe_2Ph in $[\mathbf{1}]^-$ causes a shift of about 200 mV towards negative potentials for the resulting $[Co_{11}Te_7(CO)_{10-m}(PMe_2Ph)_m]^-$ ions ($m=1-5$). As a consequence, reduction gets more difficult and oxidation easier. For these reasons traces of oxygen or water (from SiO_2) may be responsible for an oxidation, giving rise to the formation of **4**, **5**, and **6** in not very well defined ratios. Attempts to control the final oxidation by the addition of $[(C_5H_5)_2Fe]PF_6$ to the original reaction mixture did not significantly improve the yield of neutral products.

Different reaction mechanisms have been established for the substitution of CO in mononuclear metal complexes such as dissociative, associative, or interchange processes.[10] Mechanistic investigations in metal cluster compounds are difficult and therefore scarce.[10] For the same reasons it was not possible to monitor kinetically the reactions implied in the successive substitution reactions by electrochemistry. From DFT calculations on the anions $[\mathbf{1}]^{n-}$ ($n=1$, 2) a more pronounced reactivity was predicted for the monoanion,[6] and this has been confirmed by the electrochemical studies. The difference in reactivity was attributed to an increased electron density at the μ_5-Te bridges in $[\mathbf{1}]^-$, which should facilitate electron transfer and chemical reactions. Our preliminary calculations on the neutral $[Co_{11}Te_7(CO)_9(PH_3)]$ species have also shown that the μ_5-Te bridges contribute with large s and p orbital coefficients to the HOMO.

Experimental Section

All manipulations were carried out under nitrogen by using Schlenk techniques. Further information and synthetic procedures for $[Cp^*_2Nb(CO)_2]_n[Co_{11}Te_7(CO)_{10}]$ are given in reference [6].

Electrochemistry: Voltammetric analyses were carried out in a standard three-electrode cell with a Tacussel UAP4 unit cell. The reference electrode was a saturated calomel electrode (SCE) separated from the solution by a sintered glass disk. The auxiliary electrode was a platinum wire. For all voltammetric measurements, the working electrode was a vitreous carbon

electrode. The controlled potential electrolysis was performed with an Amel 552 potentiostat coupled to an Amel 721 electronic integrator. Electrolyses were performed in a cell with three compartments separated with fritted glasses of medium porosity. A carbon gauze was used as the cathode, a platinum plate was used as the anode, and a saturated calomel electrode was used as the reference electrode.

Synthesis of $[Co_{11}Te_7(CO)_6(PMe_2Ph)_4]$ (5): PMe_2Ph (140 μL, 135 mg, 0.978 mmol) was added to a brown solution of $[Cp^*_2Nb(CO)_2][Co_{11}Te_7(CO)_{10}]$ (450 mg, 0.200 mmol) in CH_2Cl_2 (70 mL). After the mixture was stirred at 20 °C for 20 h, the solvent was evaporated and the dark brown residue was washed twice with pentane. Chromatography on SiO_2 (column 10 cm, ∅3 cm) gave a broad brown band upon elution with CH_2Cl_2/toluene 1:1 which contained **5** (290 mg, 0.128 mmol, 64 %). Analytically pure brown prisms were obtained by repeated recrystallization from toluene/pentane 2:1 at −20 °C. Complex **5**: elemental analysis calcd (%) for $C_{38}H_{44}Co_{11}O_6P_4Te_7$ (2262.1): C 20.18, H 1.96, P 5.47; found: C 19.85, H 2.29, P 5.70; FD-MS (from toluene): 2263 (center); IR (KBr): $\tilde{\nu}$ = 1923s (ν(CO), br) cm^{-1}.

Reaction of $[Cp^*_2Nb(CO)_2]_2[Co_{11}Te_7(CO)_{10}]$ with PMe_2Ph: PMe_2Ph (140 μL, 135 mg, 0.978 mmol) was added to a brown solution of recrystallized $[Cp^*_2Nb(CO)_2]_2[Co_{11}Te_7(CO)_{10}]$ (250 mg, 0.09 mmol) in CH_2Cl_2 (70 mL). Reaction conditions and workup followed the procedure given for the reaction of $[Cp^*_2Nb(CO)_2][Co_{11}Te_7(CO)_{10}]$ with PMe_2Ph. Fractional crystallization of the chromatographed material (yield 180 mg, 87 %) from toluene/pentane 2:1 first gave brown prisms of **5** and then a small crop of brown needles of $[Co_{11}Te_7(CO)_5(PMe_2Ph)_5]$ (**6**). Complex **6**: elemental analysis calcd (%) for $C_{45}H_{55}Co_{11}O_5P_5Te_7$ (2372.1): C 22.78, H 2.34; found: C 23.23, H 3.00; FD-MS (from toluene): 2374 (center); IR (KBr, cm^{-1}): $\tilde{\nu}$ = 1931s, 1909vs (ν(CO)) cm^{-1}.

Attempted reaction of $[Cp^*_2Nb(CO)_2][Co(CO)_4]$ with PMe_2Ph: The yellow mixture of $[Cp^*_2Nb(CO)_2][Co(CO)_4]$ (120 mg, 0.200 mmol),[6] PMe_2Ph (140 μL, 135 mg, 0.978 mmol) and CH_2Cl_2 (50 mL) was stirred for 20 h at room temperature. After evaporation of the solvent the yellow residue was recrystallized from methanol. $[Cp^*_2Nb(CO)_2][Co(CO)_4]$ was recovered nearly quantitatively.

Crystal structure determination for 6: Flat prisms, 0.32 × 0.20 × 0.14 mm, monoclinic, $P2_1/n$, a = 11.542(1), b = 42.188(2), c = 15.013(1) Å, β = 103.25(1)°. V = 7115(1) $Å^3$, Z = 4, ρ_{calcd} = 2.332 $g\,cm^{-3}$, θ = 2.01 – 25.21°, μ = 5.460 mm^{-1}, 54747 measured reflections, 11846 independent reflections (R_{int} = 0.125), 8566 observed reflections ($I > 4\sigma(I)$), 702 refined parameters, $R1$ = 0.0363, $wR2$ = 0.0837, residual electron density 0.952/ − 1.004 e $Å^{-3}$. Data were collected at 173 K on a STOE imaging plate diffraction system. All examined crystals consisted of at least two intergrown individuals, which showed a slightly twisted orientation of the unit cells. Too much data were lost due to overlapping of the reflections when the integration of the intensities was carried out for two individuals simultaneously. Therefore the integration was carried out only for the dominant individual with as low mosaic spread and reflection width as possible. As expected, the merging R value for those data was increased but not unreasonably high. Structure solution with direct methods and the refinement of the structure were not hindered. After the empirical absorption correction (DIFABS) only some anisotropic thermal parameters were slightly enlarged, but estimated standard deviations and R values showed clearly, that the result of this structure determination was reliable.

CCDC-203183 (**6**) contain the supplementary crystallographic data for this paper. These data can be obtained free of charge via www.ccdc.cam.ac.uk/conts/retrieving.html (or from the Cambridge Crystallographic Center, 12 Union Road, Cambridge CB2 1EZ, UK; Fax: (+44) 1223-336033; or deposit@ccdc.cam.ac.uk).

Acknowledgement

We gratefully acknowledge financial support from the Deutsche Forschungsgemeinschaft. Parts of this work were supported by Deutscher Akademischer Auslandsdienst and the Ministère des Affaires Etrangères (program PROCOPE).

[1] a) J. W. Kolis, *Coord. Chem. Rev.* **1990**, *105*, 195—219; b) L. C. Roof, J. W. Kolis, *Chem. Rev.* **1993**, *93*, 1037 – 1080.

[2] a) J. F. Corrigan, D. Fenske, *Chem. Commun.* **1996**, 943—944; b) J. F. Corrigan, D. Fenske, W. P. Power, *Angew. Chem.* **1997**, *109*, 1224 – 1227; *Angew. Chem. Int. Ed. Engl.* **1997**, *36*, 1176—1179; c) J. F. Corrigan, D. Fenske, *Angew. Chem.* **1997**, *109*, 2070 – 2072; *Angew. Chem. Int. Ed. Engl.* **1997**, *36*, 1981 – 1983; d) J. F. Corrigan, D. Fenske, *Chem. Commun.* **1997**, 1837—1838; e) M. L. Steigerwald, T. Siegrist, S. M. Stuczynski, *Inorg. Chem.* **1991**, *30*, 4940 – 4945.

[3] See for example: T. Saito, *Adv. Inorg. Chem.* **1997**, *44*, 45 – 91.

[4] M. Brandl, H. Brunner, H. Cattey, Y. Mugnier, J. Wachter, M. Zabel, *J. Organomet. Chem*. **2002**, *659*, 22 – 28.

[5] a) G. Longoni, C. Femoni, M. C. Iapalucci, P. Zanello in *Metal Clusters in Chemistry*, *Vol. 3* (Eds.: P. Braunstein, L. A. Oro, P. R. Raithby), Wiley-VCH, **1999**, 1137—1158, and references therein; b) F. Calderoni, F. Demartin, F. F. de Biani, C. Femoni, M. C. Iapalucci, G. Longoni, P. Zanello, *Eur. J. Inorg. Chem*. **1999**, 663 – 671.

[6] H. Brunner, D. Lucas, T. Monzon, Y. Mugnier, B. Nuber, B. Stubenhofer, A. C. Stückl, J. Wachter, R. Wanninger, M. Zabel, *Chem. Eur. J.* **2000**, *6*, 493 – 530.

[7] R. Seidel, R. Kliss, S. Weissgräber, G. Henkel, *J. Chem. Soc. Chem. Commun*. **1994**, 2791 – 2792.

[8] R. Wanninger, Thesis, Universität Regensburg, **2000**.

[9] This assignment is supported by RDE electrolysis of neutral **4**, which exhibits three reduction waves at E_4, A_4 and B_4, respectively, at $E_{1/2}$ = − 0.36, − 0.98, and − 1.54 V.

[10] D. J. Darensbourg in *The Chemistry of Metal Cluster Complexes* (Eds.: D. F. Shriver, H. D. Kaesz, R. D. Adams), VCH Publishers, **1990**, 171 – 200.

Received: February 11, 2003 [F4841]

